Probabilistic Dominant Frequency Estimation in AF from ECGI

C Fambuena-Santos[1], I Hernández-Romero[1], C Herrero-Martín, J Reventós-Presmanes[2], E Invers-Rubio[2], L. Mont[2], AM Climent[1], MS Guillem[1]

[1]ITACA Institute, Universitat Politècnica de València, Valencia, Spain
[2]Hospital Clínic de Barcelona, Barcelona, Spain

Abstract

Non-invasive estimation of high frequency activation regions in atrial fibrillation (AF) may have an important role in patient stratification and ablation guidance. This work presents a methodology to robustly estimate DF maps in ECGI, where the uncertainty associated to the estimates is modelled making use of a set of ECGI solutions from a range of different lambda parameters (DF-LR) in Tikhonov 0-order regularization.

The proposed DF-LR method was compared to the DFs obtained from the standard L-curve (DF-LC) optimization. Specifically, the highest dominant frequency (HDF) found with both methods was tested in 2 AF simulations. In addition, the reproducibility of the DF maps was studied in a clinical case using ECGI signals from a persistent AF patient.

DF-LR method overcame the DF-LC in terms of HDF sensitivity. Furthermore, the mean absolute difference between consecutive DF maps was lower in DF-LR method (0.64±0.34Hz vs 1.38±0.11 Hz) showing higher reproducibility.

1. Introduction

There is scientific evidence demonstrating that atrial fibrillation (AF) can be originated and maintained by localized high activation frequency areas [1]. Additionally, it has been observed that the spectral content of the atrial electrical activity is well preserved in non-invasive BSPM [2]. Some studies have gone a step further and estimated dominant activation frequencies (DFs) in inverse computed electrograms (icEGMs) with good results when compared to other temporal magnitudes [3][4]. These results open the possibility of estimating highest DF (HDF) areas non-invasively, which could impact on a better AF patient stratification and better ablation planning.

The typical approach followed to estimate DF in icEGMs is by localizing the peak of maximum amplitude in the spectrum. However, this method does not consider possible uncertainty sources affecting the DF estimate, like the spatial mixing of the spectral content present when solving the inverse problem. In this work we present a methodology to robustly estimate DF maps in ECGI where the uncertainty associated to the estimates can be quantified and used to obtain more reproducible DF maps

2. Materials and Methods

2.1. Data collection and preprocessing

Two AF episodes of 10s duration were simulated using a 3-dimentional realistic geometry of the human atria. Specific distributions of electrical remodelling and slow conduction areas were included in the models to generate and maintain re-entrant propagation patterns. Electrogram signals in the epicardium were then computed from the simulated transmembrane potentials. Body surface potentials (BSPM) were obtained by solving the forward problem of electrocardiography with the boundary element method. Finally, gaussian noise was added to the resultant BSPM with a signal to noise ratio of 20 dB and a 0.5-20 Hz bandpass filter was applied to improve signal quality. In addition to the simulated data, BSPM signals of a persistent AF patient (female, 70 years old) were recorded before PVI using 128 electrodes. Both torso geometry and electrode positions were recorded by photogrammetry. The atrial anatomy and fibrosis distribution were obtained from a late gadolinium enhancement MRI (LGE-MRI).

2.2. Inverse problem and dominant frequency estimation

We solved the inverse problem by applying 0-order Tikhonov regularization. With this procedure, inverse computed electrograms (icEGMs) were obtained for 41 different regularization parameters (λ) in the range [10^{-12}, 10^{-2}]. Dominant frequency (DF) maps were computed for each of these solutions. The DF was considered as the peak with maximum amplitude in the spectrum, which was calculated using Welch's periodogram with a Hamming window of 4s length and 50% overlap.

Pearson correlation coefficients between DF maps

from consecutive λ values were computed together with the normalized power within the 0.5-12 Hz band for each of the 41 sets of spectra calculated. A range of λ values with consistently high correlations and power spectral ratios was manually selected, and their corresponding icEGMs were used to compute the final DF. A probability density function was obtained by fitting a gaussian mixture model to the DF values computed from the selected icEGMs. The final estimation probability was calculated using equation (1) in an interval of ±0.2Hz around the DF estimate.

$$p(x) = \sum_{k=1}^{n} \alpha_k \cdot N(x|\mu_k, \sigma_k) \qquad (1)$$

where α_k is the probability of a DF value to belong to a particular population of frequencies following a gaussian distribution, μ_k is the mean of each gaussian distribution and σ_k is the standard deviation. The DF associated to each atrial location was estimated as the peak with maximum amplitude in this probability density function.

Finally, the L-curve methodology was applied to determine the optimal lambda and rescue its DF map (LC) [5]. This map was compared to the final DF estimate obtained using the lambda-range (LR) approach explained above.

2.3. Evaluation of Dominant Frequency Estimation Methods

In simulations, the gold standard activation frequency was determined by counting the activations present in the computed transmembrane potentials. To compare the performance between the proposed LR method and the standard LC in the context of a clinical application, we calculated the highest dominant frequency (HDF) regions with both methods and compared with the gold standard. HDFs were segmented using a custom region growing algorithm adapted for 3D data. This algorithm allowed us to segment all the different regions with similar DF values. The HDF in each map was obtained as the set of regions containing any of the frequencies present above the 90-percentile interval. We quantified the sensitivity and specificity of the HDF regions obtained with both methods.

Temporal reproducibility of the DF maps obtained from the patient was quantified by splitting the 30 second ECGI signals into 10s windows with 50% overlap. The mean absolute difference between DF maps from consecutive windows was computed in three scenarios: using CL maps, LR maps containing DFs values from all the atria and LR maps with only the atrial nodes presenting an estimation probability higher than 0.7.

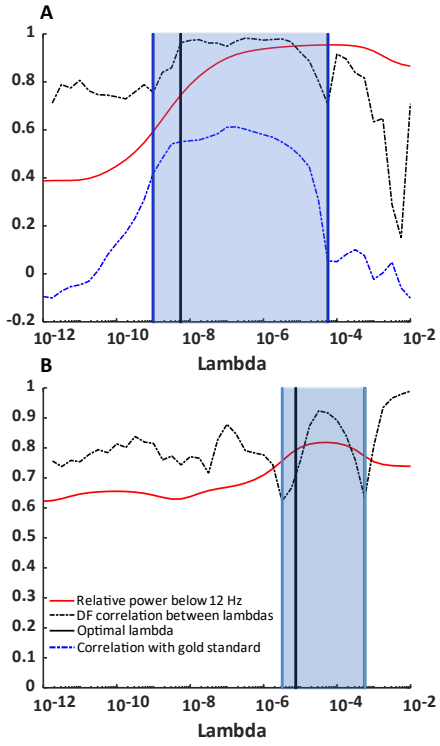

Figure 1. A) Lambda range selected to compute DF map in simulation 2. This range was adjusted to include a high power ratio in the frequency band of interest and a consistently high correlation between DF maps of consecutive lambdas. B) Lambda range selected in a patient recording using the same approach.

3. Results

3.1. Lambda Range selection

In the simulated AF episodes we selected the range of λ values (10^{-9} to $5.62 \cdot 10^{-5}$) that maximized the power ratio within the 0.5-12 Hz band and the correlation between DF maps from consecutive λ values. In this range, the correlation with the gold standard activation frequency is also maximized. The λ value selected by the L-curve optimization method lies withing this same range, and close to its lower boundary. In panel B, we can see the same analysis applied to the clinical data. In this case, maximization of both, the power within the interest frequency band and the correlation between DFs from consecutive λ values lies within the $3 \cdot 10^{-6}$ to $3 \cdot 10^{-4}$ range, a narrower interval than the one obtained for the simulations. The lambda value selected by the L-curve optimization is again within this range.

3.2. DF Evaluation

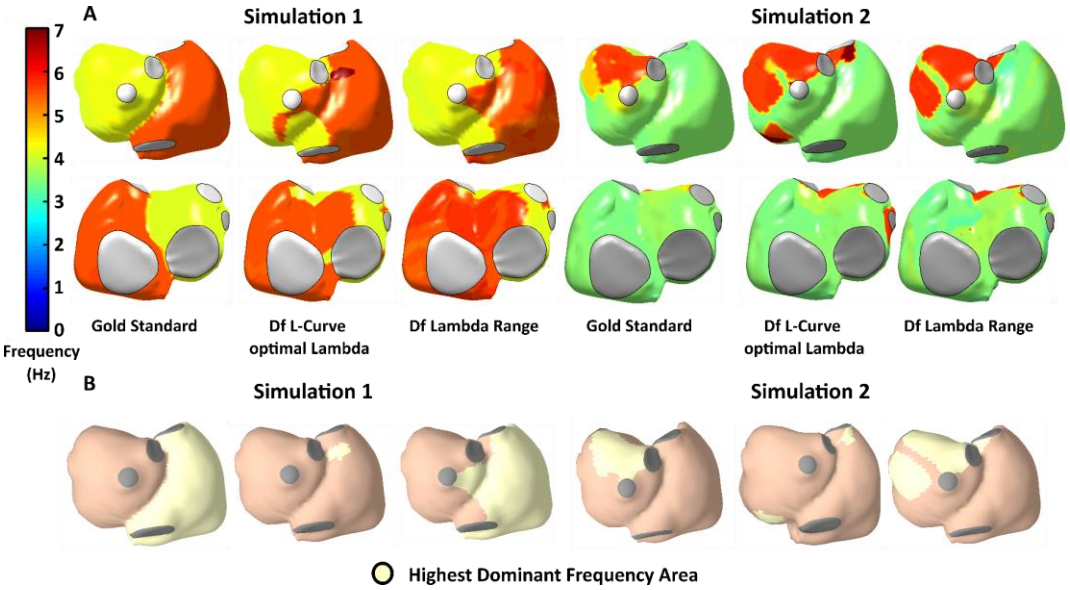

Figure 2. A) Posterior and anterior views of the of the OLC, LR and gold standard DF maps. The 3 first columns correspond to the first simulation, and the 3 last to the second. B) HDF areas obtained for simulation 1 and 2.

DF maps obtained by LC and LR methods, together with the gold standard are depicted in Fig.2. Both methods showed similar distributions of the largest DF areas in both simulations, but our LR method outperforms the LC method. In simulation 1, where the gold standard shows two different activation frequencies in each atria, the LC method presents a wider penetration of the right atrial activation frequency into the left atrium, right below the right inferior pulmonary vein. Similarly, in simulation 2, the HDF is incorrectly estimated to appear near the mitral valve. More importantly, both simulations show small and localized regions of HDFs higher than the gold standard HDF: the posterior wall of the right atrium in simulation 1 and the superior vena cava and the mitral valve in simulation 2. The presence of these artifactual HDFs in the LC method yield to a poor HDF estimation as compared to the LR method (see Table 1).

	Sensitivity		Specificity	
Methods	OLC	LR	OLC	LR
Sim. 1	0.010	0.929	0.995	0.782
Sim. 2	0.000	0.889	0.984	0.920

Table 1. Sensitivity and specificity of the LC and LR methods for each of the simulations.

3.3. DF estimation probability

In Fig.3, DF estimation probability maps are shown. In both simulations, there is a general drop of the probability in the boundaries between different DF regions. This observation would be consistent with the occurrence of mixing of the spectral content in the vicinity of two different DF regions.

Another area with a high uncertainty in both simulations is the septum. This is a specially challenging region for the inverse problem due to the concavity present in the area, which can be a factor leading to also to a higher spatial mixing of frequencies.

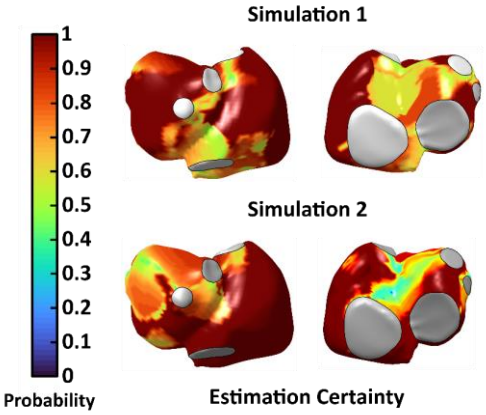

Figure 3. Estimation certainty maps within a ±0.2Hz interval around the DF estimated by our LR method.

3.3. DF estimation in patient data

The estimated DF maps in the patient data are shown in Fig.4, where the HDF area was found below the left inferior pulmonary vein, which was consistent in all the 5 windows analyzed. The estimation probability map also presents high estimation probabilities in the HDF region. This high probability was observed in all the windows, suggesting a good temporal reproducibility of the HDF. This HDF area also co-localizes with the biggest fibrotic

patch in the LGE-MRI.

Temporal stability of DF maps is shown in Fig.4.D. Differences between DF estimation in consecutive windows was larger in the LC method than in the LR method (1.38±0.11 Hz vs. 1.16±0.09 Hz) and goes down to 0.64±0.34 Hz if just high confidence regions (probability>0.7) are considered.

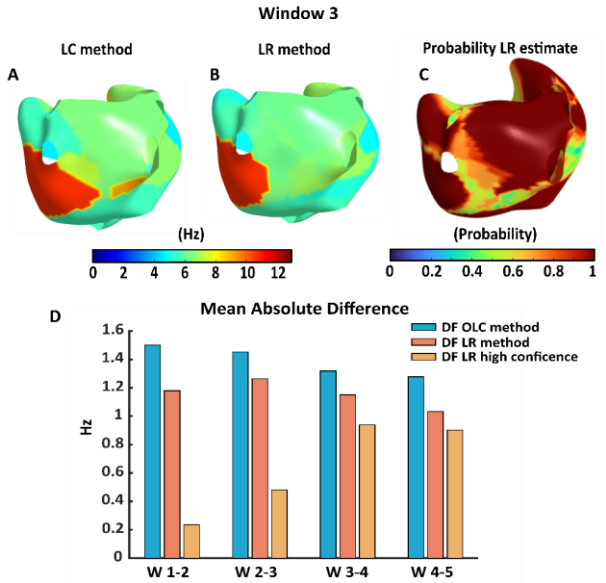

Figure 4. A and B, DF maps obtained in window 3 with LC and LR methods respectively. C, estimation probability map provided by the LR method within an interval of ±0.2Hz. D, mean absolute difference of DF maps in consecutive time windows.

4. Discussion and Conclusions

This study presents a new methodology for DF estimation in ECGI which includes an alternative approach to find the optimal regularization parameters. Additionally, a probabilistic framework that makes use of information from a range of ECGI solutions is used to quantify the uncertainty of the estimates. This methodology provides more reproducible DF maps than the state of the art methods.

Both, in simulations and patient data, the optimal lambda value found by the L-curve lied into our proposed lambda range, although a narrower lambda range was obtained for the patient data. A possible explanation for this is the existence of additional uncertainty sources which are not present in simulations, like anatomical deformations or movements.

Artifactual HDF areas, corresponding to harmonic frequencies of actual DFs appear when using the LC method. Although they can be easily identified in computer simulations, when coming to patient data we do not have a gold standard to rule out these contributions. We have shown that our LR method may allow to overcome this limitation inherent to DF estimation in AF signals.

Regarding the limitations of the study, the lambda range used for the DF estimation was manually selected by an operator. In the future we plan to automatize this step based on the spectral parameters found. Additionally, no intracavitary information of the AF patient was used to confirm the location of the highest DF site.

Overall, our results suggest that, in addition to the L-curve, other spectral parameters can be used to regularize the inverse problem for DF estimation. Furthermore, the optimal solution found with the L-curve may be improved when making use of a set of solutions with different λ values, providing additional information on the estimation uncertainty.

Acknowledgments and Conflict of interests

This work was supported by PersonalizeAF project. This project has received funding from the European Union's Horizon 2020 research and innovation program under the Marie Skłodowska-Curie grant agreement No 860974. This publication reflects only the author's view and the Agency is not responsible for any use that may be made of the information it contains.

AMC, MSG and IHR are co-founders and shareholders of Corify Care SL.

References

[1] Mandapati R, Skanes A, Chen J, Berenfeld O, Jalife J. Stable microreentrant sources as a mechanism of atrial fibrillation in the isolated sheep heart. Circulation. 2000;101(2):194–9.

[2] Guillem MS, Climent AM, Millet J, Arenal Á, Fernández-Avilés F, Jalife J, et al. Noninvasive localization of maximal frequency sites of atrial fibrillation by body surface potential mapping. Circ Arrhythmia Electrophysiol. 2013;6(2):294–301.

[3] Pedrón-Torrecilla J, Rodrigo M, Climent AM, Liberos A, Pérez-David E, Bermejo J, et al. Noninvasive estimation of epicardial dominant high-frequency regions during atrial fibrillation. J Cardiovasc Electrophysiol. 2016;27(4):435–42.

[4] Rodrigo M, Climent AM, Liberos A, Fernández-Avilés F, Berenfeld O, Atienza F, et al. Highest dominant frequency and rotor positions are robust markers of driver location during noninvasive mapping of atrial fibrillation: A computational study. Hear Rhythm. 2017;14(8):1224–33.

[5] Hansen PC, O'Leary DP. The Use of the L-Curve in the Regularization of Discrete Ill-Posed Problems. SIAM J Sci Comput. 1993;14(6):1487–503.

Address for correspondence:

Carlos Fambuena Santos.
ITACA. Edificio 8G acceso B. Universitat Politècnica de València. Camino de Vera s/n. 46022 Valencia, Spain.
carfamsa@upvnet.upv.es